



# Attention-Related Brain Activation Is Altered in Older Adults With White Matter Hyperintensities Using Multi-Echo fMRI

Sarah Atwi<sup>1,2\*</sup>, Arron W. S. Metcalfe<sup>1,3</sup>, Andrew D. Robertson<sup>1</sup>, Jeremy Rezmovitz<sup>4</sup>, Nicole D. Anderson<sup>5,6</sup> and Bradley J. MacIntosh<sup>1,2</sup>

<sup>1</sup> Heart and Stroke Foundation Canadian Partnership for Stroke Recovery, Sunnybrook Research Institute, University of Toronto, Toronto, ON, Canada, <sup>2</sup> Department of Medical Biophysics, University of Toronto, Toronto, ON, Canada, <sup>3</sup> Centre for Youth Bipolar Disorder, Sunnybrook Research Institute, University of Toronto, Toronto, ON, Canada, <sup>4</sup> Department of Family and Community Medicine, Sunnybrook Health Sciences Centre, Toronto, ON, Canada, <sup>5</sup> Department of Psychiatry and Psychology, University of Toronto, Toronto, ON, Canada, <sup>6</sup> Rotman Research Institute, Baycrest Centre, University of Toronto, Toronto, ON, Canada

## OPEN ACCESS

### Edited by:

Andrei Surguchov,  
University of Kansas Medical Center,  
United States

### Reviewed by:

Sofya N. Morozova,  
Research Center of Neurology, Russia  
Quanjing Chen,  
University of Rochester, United States

### \*Correspondence:

Sarah Atwi  
sarah.atwi@sunnybrook.ca

### Specialty section:

This article was submitted to  
Neurodegeneration,  
a section of the journal  
Frontiers in Neuroscience

Received: 27 February 2018

Accepted: 28 September 2018

Published: 18 October 2018

### Citation:

Atwi S, Metcalfe AWS,  
Robertson AD, Rezmovitz J,  
Anderson ND and MacIntosh BJ  
(2018) Attention-Related Brain  
Activation Is Altered in Older Adults  
With White Matter Hyperintensities  
Using Multi-Echo fMRI.  
Front. Neurosci. 12:748.  
doi: 10.3389/fnins.2018.00748

Cognitive decline is often undetectable in the early stages of accelerated vascular aging. Attentional processes are particularly affected in older adults with white matter hyperintensities (WMH), although specific neurovascular mechanisms have not been elucidated. We aimed to identify differences in attention-related neurofunctional activation and behavior between adults with and without WMH. Older adults with moderate to severe WMH ( $n = 18$ , mean age = 70 years), age-matched adults ( $n = 28$ , mean age = 72), and healthy younger adults ( $n = 19$ , mean age = 25) performed a modified flanker task during multi-echo blood oxygenation level dependent functional magnetic resonance imaging. Task-related activation was assessed using a weighted-echo approach. Healthy older adults had more widespread response and higher amplitude of activation compared to WMH adults in fronto-temporal and parietal cortices. Activation associated with processing speed was absent in the WMH group, suggesting attention-related activation deficits that may be a consequence of cerebral small vessel disease. WMH adults had greater executive contrast activation in the precuneus and posterior cingulate gyrus compared to HYA, despite no performance benefits, reinforcing the network dysfunction theory in WMH.

**Keywords:** white matter hyperintensities, small vessel disease, attention, multi-echo, fMRI, BOLD

## INTRODUCTION

Growing neuroanatomical and behavioral evidence suggests CSVD contributes to subclinical neurological deficits, but the underlying neurofunctional correlates remain unclear. CSVD is a prevalent disorder with detrimental effects on the cerebrovasculature, brain tissue, cognition, and behavior (Wardlaw et al., 2013). This insidious disease increases the risk of stroke and

**Abbreviations:** ANOVA, analysis of variance; BOLD, blood oxygenation level dependent; CSVD, cerebral small vessel disease; DSCT, Digit Symbol Coding Test; FEAT, FMRIB Expert Analysis Tool; FLAIR, Fluid Attenuated Inversion Recovery; fMRI, functional magnetic resonance imaging; HOA, healthy older adults; HYA, healthy younger adults; MNI, Montreal Neurological Institute; MoCA, Montreal Cognitive Assessment; MRI, magnetic resonance imaging; RETROICOR, Retrospective Correction Technique; S, Signal Intensity; T2\*, relaxation time; TE, echo time; TR, repetition time; WMH, white matter hyperintensities.

dementia (Snowdon et al., 1997; Vermeer et al., 2003; Barnes et al., 2013) and is responsible for myriad alterations in arteriolar, capillary and venular beds (Pantoni, 2010). A consensus of neuroanatomical imaging identifies WMH of presumed vascular origin, seen on T2-weighted MRI, as the most common hallmark of CSVD (Rost et al., 2010; Wardlaw et al., 2013). WMH impact not only the physiology of white matter (Makedonov et al., 2013) but also the anatomy and physiology of gray matter (O'Sullivan et al., 2002; Zheng et al., 2006; Bastos-Leite et al., 2008; Fu et al., 2014; Wagner et al., 2015; Shi et al., 2016).

Cognitive assessments reveal detrimental associations between CSVD and multiple behavioral domains. WMH volume is inversely related to cognitive function, globally (de Groot et al., 2000; Schmidt et al., 2004; Kerchner et al., 2012), and to processes of attention in particular (Ishikawa et al., 2012), including executive function (Breteler et al., 1994; Wright et al., 2008; Zheng et al., 2012). Attention-related dysfunction can be identified using the attention network test, which elicits brain-wide cognitive engagement using a flanker task with graded difficulty (Fan et al., 2005, 2002). Functional neuroimaging techniques that probe brain and behavior relationship in tasks of increasing difficulty may play an important role in advancing our understanding of subclinical features of WMH.

CSVD has been linked to lower functional coupling and coherence, using electroencephalography, which was reflected in lower speed of information processing (Dey et al., 2016). BOLD is a functional MRI (fMRI) approach which can probe CSVD by characterizing neurovascular signal patterns that may relate to impaired dorsal attention, default mode and fronto-parietal control networks (Spreng et al., 2013). To date, however, task-based fMRI among adults with WMH has produced conflicting findings; both increased and decreased activation are reported in attentional neural networks (Nordahl et al., 2006; Venkatraman et al., 2010; Hedden et al., 2012; Lockhart et al., 2015; Gold et al., 2017). Despite the utility of BOLD fMRI, challenges exist in the context of aging that influence signal-to-noise ratio and specificity of activation, be they physiological, neurovascular, or metabolic (Huettel et al., 2001). BOLD fMRI analysis is mature, with strategies in place to isolate and minimize physiological sources of non-interest to increase detection of neurovascular activation (Hu et al., 1995; Biswal et al., 1996; Wowk et al., 1997; Glover et al., 2000; Birn et al., 2006; Caballero-Gaudes and Reynolds, 2016). An important gap in the literature involves the limited evaluation of targeted data denoising techniques in fMRI studies probing cerebrovascular pathology, which is likely due to a greater focus on the structural changes associated with cerebrovascular dysfunction, rather than functional changes.

Improved paradigm, acquisition, and data-scrubbing strategies are likely to advance fMRI in CSVD research. The current study incorporates each of these elements as part of the experimental design, namely multi-echo fMRI during a modified attention network test (Fan et al., 2005). Multi-echo fMRI aggregates multiple image volumes to improve image quality (Posse et al., 1999; Poser et al., 2006; Kundu et al., 2013), reduces susceptibility-related signal loss (Kirilina et al., 2016), enhances anatomical-functional registration (Kundu et al., 2015), and filters high frequency artifacts (Olafsson et al., 2015). By

acquiring echo-planar images at multiple echo times, it is possible to reconstruct images in combination to accentuate particular image contrasts, although a weighted-echoes approach is most common (Posse et al., 1999). Multi-echo fMRI outperforms conventional fMRI during rapid event-related tasks (Gonzalez-Castillo et al., 2016; Lombardo et al., 2016). This is likely due to improvements in statistical power of task-related data, both at the individual and group level analysis, and by mitigating motion artifact signals, a central hindrance to producing robust BOLD data (Buur et al., 2008, 2009; Witt et al., 2016; Kundu et al., 2017).

The primary purpose of the current study was to compare widespread task network and executive network activation in response to an attention-demanding task across three groups of adults. We hypothesized that multi-echo fMRI would show marked activation and behavioral performance differences in older adults with WMH relative to age-matched healthy adults and younger healthy adults. Given that multi-echo fMRI has not been used in CSVD to date, we also consider its performance relative to the established Retrospective Correction of Physiological Motion Effects (RETROICOR) method (Glover et al., 2000).

## MATERIALS AND METHODS

### Participants

This study recruited community-dwelling individuals, comprising of healthy younger individuals (HYA), HOAs with minimal WMH lesion burden (HOA), and older adults with moderate to severe lesion burden (WMH). Most participants were recruited through community advertising. A portion of WMH adults was recruited through a Family Medicine clinic mail-out, which targeted patients with one or more vascular risk factors. Exclusion criteria included contraindications to MRI, a score below 21 on the Montreal Cognitive Assessment (MoCA), and a self-reported history of type 2 diabetes requiring insulin, cardiopulmonary illness, stroke, or dementia. WMH severity was indexed by the Fazekas rating scale from 0 to 3 using the following rubric: 0 – no periventricular or deep white matter WMH; 1 – pencil-thin lining or capped periventricular WMH and/or punctate foci in deep white matter; 2 – smooth periventricular WMH halo and/or beginning of deep WMH confluence; and 3 – irregular periventricular signal extending to deep white matter and/or large deep white matter confluence (Fazekas et al., 2002). Those with Fazekas  $\geq 2$  were assigned to the WMH group. All older participants performed the Digit Symbol Coding Test (DSCT), as well as the MoCA. This study was approved and carried out in accordance with the recommendations of the Sunnybrook Healthy Sciences Centre Research Ethics Board with written informed consent from all subjects. All subjects gave written informed consent in accordance with the Declaration of Helsinki. The Sunnybrook Healthy Sciences Centre Research Ethics Board approved the protocol. A total of 65 participants, including 19 HYA [10 female, age (mean  $\pm$  SD) 25  $\pm$  1 years], 28 HOA (17 female, 70  $\pm$  6 years), and 18 WMH (10 female, 72  $\pm$  5 years) were MRI eligible and agreed to participate, received brain MRI, and

**TABLE 1** | Group demographics and clinical characteristics.

	HYA, <i>n</i> = 19	HOA, <i>n</i> = 28	WMH, <i>n</i> = 18
Age, years	25 ± 3	70 ± 6	72 ± 5
Sex, F:M	10:9	17:11	10:8
Education, years	17 ± 2	17 ± 3 <sup>a</sup>	17 ± 2
MoCA, total score (range)	–	26 ± 2 (23–30) <sup>a</sup>	25 ± 2 (22–29) <sup>b</sup>
DSCT total score (range)	–	67 ± 14 (14–89)	56 ± 11(27–70) <sup>b</sup>
WMH volume, ml	–	0.71 ± 0.6 <sup>b</sup>	9.21 ± 0.6
Hypertension, count (%)	0	0(0)	4(22)
Type II Diabetes Mellitus, count (%)	0	1(4)	1(6)

Data are expressed as mean ± standard deviation or *n* (%). MoCA, Montreal Cognitive Assessment; DSCT, Digit Symbol Coding Test; WMH, white matter hyperintensities; a, *n* = 27; b, *n* = 17.

underwent cognitive testing. The groups were well matched in terms of years of education ( $F = 0.52$ ,  $df = 2,64$ ,  $P = 0.47$ ), sex ( $\chi^2 = 0.8$ ,  $df = 2,64$ ,  $P = 0.7$ ). The older groups were age matched ( $W = 193$ ,  $P = 0.19$ ) and MoCA total score was not different ( $W = 301$ ,  $P = 0.083$ ). Additional demographic details, including a group difference in WMH volumes ( $W = 24$ ,  $P < 0.001$ ) are provided in **Table 1**.

## MRI Acquisition

Images were acquired using a 3T scanner (Achieva, Philips Healthcare, Best, Netherlands) with an 8-channel head coil receiver. High-resolution 3D T1-weighted anatomical images were acquired using the following parameters: repetition time (TR) = 9.5 ms, echo time (TE) = 2.3 ms, 140 slices, flip angle = 8°, voxel dimensions = 0.63 × 0.63 × 1.2 mm. Fluid-attenuated inversion recovery (FLAIR) images were acquired in 2D with T2-weighting to assess WMH lesions using the following parameters: TR = 9000 ms, TE = 125 ms, 52 slices, flip angle = 90°, voxel dimensions = 0.43 × 0.43 × 3 mm. The multi-echo BOLD acquisition was 7 min and 5.5 s in duration (TR = 2300 ms, 185 volumes) and involved the following parameters: three consecutive echoes per volume at TE = 13.82, 35.35, and 56.89 ms, 28 slices, flip angle = 70°, and voxel dimensions = 2.88 × 2.88 × 4 mm. Heart rate and breathing rate were monitored using pulse oximetry and respiratory bellows, respectively.

## WMH Volume Quantification

Gray matter, white matter and cerebrospinal fluid were segmented on the T1-weighted image using FMRIB Automated Segmentation Tool (Zhang et al., 2001). WMH were segmented on the FLAIR images using in-house software, a fuzzy lesion extractor (Gibson et al., 2010). Two experienced and blinded raters [Sarah Atwi and Andrew D. Robertson] performed Fazekas ratings. Inter-rater reliability was 87%, and discrepancies in scoring were discussed to achieve consensus. A FLAIR image was not acquired for one older adult; however, they were classified as an HOA due to lack of WMH features in the T1-weighted image.

## Task fMRI

The attention network test is a flanker paradigm that probes attention and psychomotor speed (Fan et al., 2005). The event-related task design was implemented using E-Prime v1.2 (Psychology Software Tools, Pittsburgh, PA, United States) and consisted of 12 in-scanner practice trials with feedback (requiring 100% accuracy on the final 6 trials) and 120 experimental trials during fMRI. In addition, participants performed a shortened practice test using a keyboard response triggers immediately prior to MRI scanning. Participants used right and left hand, index finger response triggers to identify the direction of the middle arrow (i.e., respond using the same hand as the direction of the middle arrow), while four flanking arrows pointed congruently, or incongruently in the direction of the target (e.g., congruent condition: →→→→→, ←←←←←; incongruent condition: →→←→→, ←←→←←). The arrows were presented above or below a centralized fixation cross, which appeared for 150 ms at the onset of each trial, and were counterbalanced across conditions. On two-thirds of trials, a warning cue appeared for 400 ms, above, below, or superimposed upon the fixation cross; all other trials received continued 400 ms of fixation. At 550 ms post-onset, the flankers and target were presented for 1550 ms. The post-target fixation period was 660 ms. Inter-trial intervals ranged from 0 to 7360 ms (mean = 900 ms) during which the fixation was always present. The event-related contrast used low-level fixation as the baseline to test widespread task network engagement. A higher-level *executive* contrast was studied by analyzing incongruent task activation versus low-level fixation baseline minus congruent task activation versus low-level fixation baseline. With- and without-cue flanker conditions were included in the *executive* contrast to maximize the number of trials.

## Functional Image Post-processing and Time Series Analysis

Multi-echo BOLD data were combined using a weighting scheme first described by Posse et al. (1999), and later detailed by Poser et al. (2006). This approach weights the signal intensities (*S*) from each echo time image by using the summation of data acquired at different echo times ( $TE_n$ ) at each TR multiplied by a weighted function that uses the derived relaxation time ( $T_2^*$ ):

$$\text{Weighted Echoes Signal} = \sum_{n=1}^N S(TR, TE_n) \left( \frac{TE_n}{T_2^*} \exp\left(-\frac{TE_n}{T_2^*}\right) \right)$$

For comparison, we also processed the second echo (TE = 35.35 ms) alone to emulate a single-echo analysis, which included a retrospective correction of physiological motion effects (RETROICOR) (Glover et al., 2000). fMRI processing was carried out on the weighted-echo, RETROICOR, and uncorrected single-echo (TE = 35.35) versions of the fMRI data, as described in Section “BOLD Processing Comparison.”

We used FMRIB software library Version 5.0 for fMRI analysis. The Linear Image Registration Tool (FLIRT) was used to correct for head motion, the Brain Extraction Tool was used to extract brain from skull (Smith, 2002), and the Expert Analysis Tool (FEAT) was used to spatially smooth with a 6-mm Gaussian

kernel, intensity normalize by a single multiplicative factor, and temporally filter (high-pass) equivalent to 50 s (Jenkinson et al., 2002). Functional data were registered to the T1-weighted image using 6 degrees of freedom (Greve and Fischl, 2009). Registration of the T1-weighted image to Montreal Neurological Institute space with 2-mm isotropic resolution was carried out using FLIRT (Jenkinson and Smith, 2001; Jenkinson et al., 2002) and was refined using FNIRT non-linear registration (Andersson et al., 2007). Participants' head motion was inspected by the mean frame-wise displacement and those with a mean displacement below 0.4 mm were included in the analysis.

Time-series statistical analysis was carried out using FEAT to create a general linear model with local autocorrelation correction. The behavioral task patterns were convolved with a double gamma hemodynamic response function. The main contrasts of interest include only correct trials during: (1) *all versus baseline* conditions and (2) *executive* contrast (i.e., incongruent versus congruent conditions).

## BOLD Processing Comparison

To examine the utility of multi-echo fMRI, we compared the weighted-echoes and single-echo RETROICOR approaches to the uncorrected single-echo data. The within-subject comparisons were based on Z-statistic maps from the *all versus baseline* task contrast, without adjustment for reaction time. We calculated the slope of a line of best fit through voxel-wise data from each post-processing approach versus the uncorrected single-echo reference for each participant (i.e., weighted-echoes Z-stat map versus single-echo Z-stat map; RETROICOR Z-stat map versus single-echo Z-stat map; representative participant in **Figure 1A**). A slope of 1 signifies the post-processing approach yields equivalent Z-values compared to the uncorrected single-echo analysis. A slope less than 1 indicates Z-values are lower than an uncorrected single-echo analysis, and a slope above 1 would signify higher Z-values in this voxel-by-voxel comparison.  $R^2$  values from the linear association between RETROICOR and single-echo and between weighted-echoes and single-echo were compared. Group differences in slope and  $R^2$  values for both method comparisons were assessed. Given that multi-echo fMRI and RETROICOR are able to reduce spurious signals, this analysis would help support hypothesis testing using the weighted-echoes data.

## Statistical Analysis

Group differences for sex, hypertension, and diabetes mellitus were assessed using Pearson's Chi-squared test. Group differences for education, task reaction time, and task accuracy were assessed using one-way ANOVA and *post hoc* pairwise comparison with Tukey's adjustment for multiple comparisons. Differences between HOA and WMH for age, DSCT, MoCA, and WMH volume were assessed using a Wilcoxon rank sum test. These tests were performed using R software (V3.1.1) and significant differences were inferred at  $P < 0.05$ .

fMRI processing methods were compared using a Welch two sample *t*-test of the slope and  $R^2$  values from the linear associations between RETROICOR and single-echo Z-stats, and between from the weighted-echoes and single-echo Z-stats.

Differences between each method and the single-echo method were assessed using a one-sample *t*-test comparing the slopes to 1. Group differences in slope and  $R^2$  values were analyzed using a one-way ANOVA and *post hoc* pairwise comparison with Tukey's adjustment for multiple comparisons.

Using the weighted-echoes fMRI, a group analysis was performed using only correct trials during the task. We identified regions of interest based on a voxel-level threshold of  $Z > 2.32$  ( $P < 0.01$ ) followed by a cluster-level threshold of  $P < 0.05$ . This approach accounts for family wise error and was implemented as a mixed effects model using FMRIB's Local Analysis of Mixed Effects (stage 1 + 2), which estimates the higher-level parameter estimates and mixed effects variance for group comparisons (Beckmann et al., 2003; Woolrich et al., 2004). We tested for an effect of group and subsequent paired group differences after inspecting single group average maps using FEAT. In addition to uncorrected results, we adjusted brain activation for performance using mean of correct trial reaction times during *all conditions*. Comparison of reaction times and percent BOLD signal changes was studied during the *all versus baseline*, *incongruent*, and *congruent* conditions. Signal within significant clusters from the unadjusted all-group's average maps of each condition was independently compared to respective reaction times and accuracy using Pearson-product moment correlation.

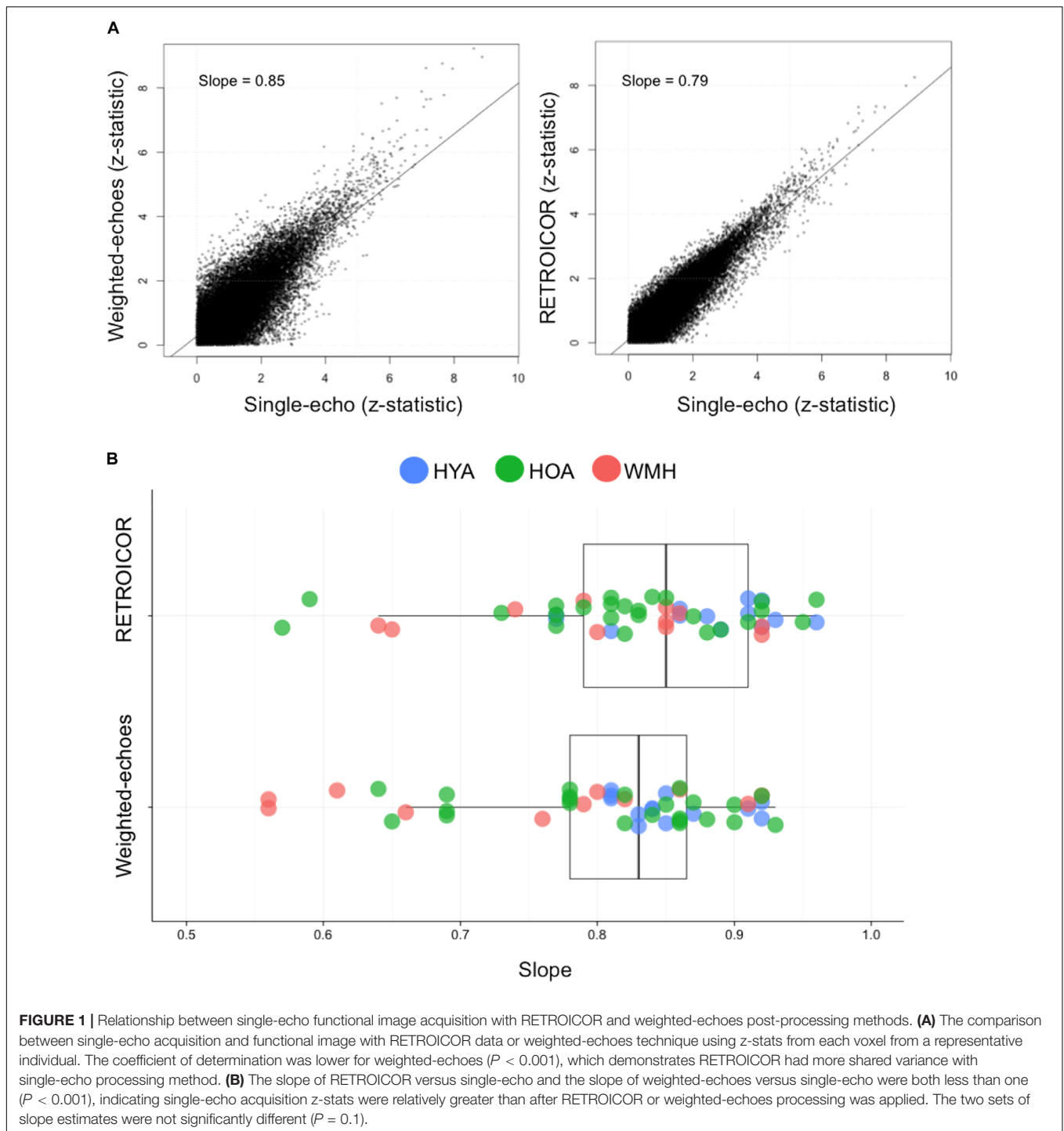
## RESULTS

### Group Characteristics

Clinical and demographic information for participants are presented in **Table 1**. The WMH group had a lower DSCT scores ( $W = 376.5$ ,  $P = 0.0001$ ) and higher prevalence of hypertension ( $P = 0.04$ ) compared to HOA.

### Multi-Echo Versus RETROICOR Comparison

Seven WMH, 4 HOA, and 6 HYA were omitted from the methods comparison due to incomplete heart rate and ventilation rate log files, precluding the RETROICOR processing. Relative to the uncorrected single-echo fMRI, voxel-wise Z-stats from the weighted-echo method produced a slope of  $0.80 \pm 0.1$ , and the RETROICOR method produced a slope of  $0.83 \pm 0.09$ ; these slopes were not different from one another ( $t = -1.6$ ,  $df = 91.7$ ,  $P = 0.1$ ) (**Figure 1**). The slopes were, however, less than unity, indicating both approaches tend to reduce Z-stat values (weighted-echo:  $t = -13.0$ ,  $df = 47$ ,  $P < 0.001$ ; RETROICOR:  $t = -12.9$ ,  $df = 47$ ,  $P < 0.001$ ).  $R^2$  values from the association between the weighted-echo and single-echo Z-stats were lower than those from the association between RETROICOR and single-echo Z-stats ( $t = -4.0$ ,  $P < 0.001$ ). Weighted-echoes versus single echo slope were different between groups ( $F = 3.1$ ,  $df = 2,47$ ,  $P = 0.05$ ), where HYA had higher slopes than WMH ( $P = 0.04$ ), but  $R^2$  values did not differ between groups ( $F = 2.8$ ,  $df = 2,47$ ,  $P = 0.07$ ). RETROICOR versus single-echo slopes did not differ between groups ( $F = 2.3$ ,  $df = 2,47$ ,  $P = 0.1$ ), but  $R^2$  values were significantly different ( $F = 4.1$ ,  $df = 2,47$ ,  $P = 0.02$ ), in that HYA had higher  $R^2$  compared to WMH ( $P = 0.02$ ). The



weighted-echo maps showed lower spatial dispersion of signal comparative to RETROICOR (see **Supplementary Figure S1**).

## Behavioral Results

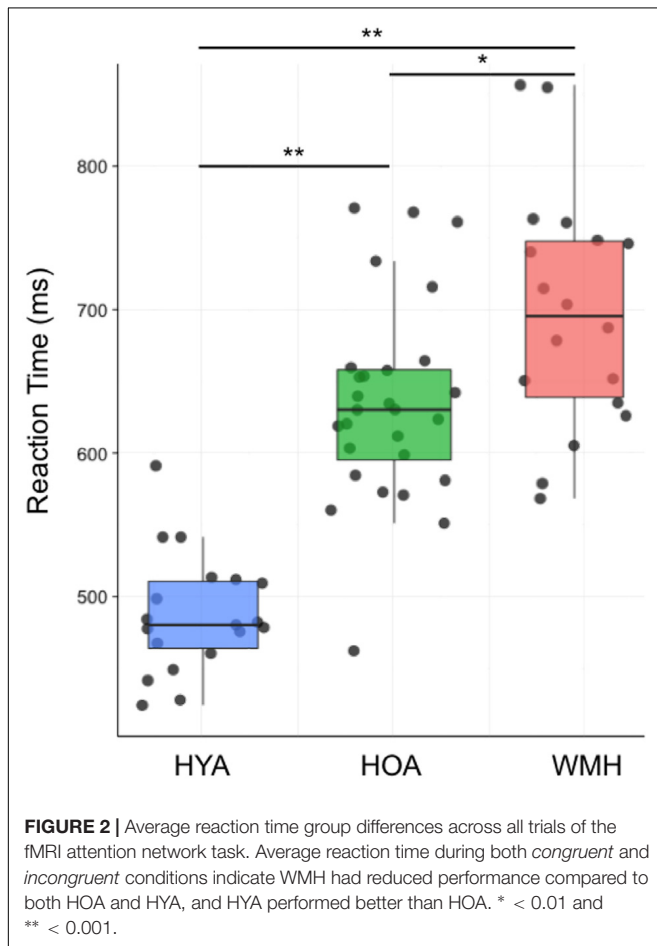
Across all trials, accuracy was not different between groups (**Table 2**;  $F = 0.4$ ,  $df = 2,64$ ,  $P = 0.7$ ). When considering only the correct trials, there was a main effect of group on reaction time ( $F = 49.2$ ,  $df = 2,64$ ,  $P < 0.0001$ ) (**Figure 2**). HYA had

shorter reaction times than both HOA and WMH ( $P < 0.001$ ), and HOA had shorter reaction times than WMH ( $P < 0.01$ ) (**Table 2**). Similarly, group differences in reaction time were observed for all correct *congruent* and *incongruent* tasks (i.e., including trials with- and without- cues) (congruent:  $F = 45.04$ ,  $df = 2,64$ ,  $P < 0.001$ ; incongruent:  $F = 49.2$ ,  $df = 2,64$ ,  $P < 0.001$ ) where HYA had lower reaction times compared to HOA and WMH (congruent:  $P < 0.001$ ; incongruent:  $P < 0.001$ ), and

**TABLE 2** | Reaction time and accuracy of attention network test during fMRI scan.

	HYA	HOA	WMH
<b>All conditions</b>			
Reaction time, ms	487.2 ± 41.5	634.8 ± 69.5	698.3 ± 83.5
Accuracy, %	98.6 ± 1.1	98.8 ± 1.9	98.3 ± 1.8
<b>Congruent</b>			
Reaction time, ms	456.6 ± 39.0	600.7 ± 71.0	657.8 ± 83.2
Accuracy, %	99.4 ± 1.0	99.3 ± 1.3	98.4 ± 2.2
<b>Incongruent</b>			
Reaction time, ms	517.9 ± 46.2	668.9 ± 71.3	738.8 ± 86.7
Accuracy, %	97.7 ± 1.9	98.3 ± 2.6	98.2 ± 1.8
<b>Executive contrast</b>			
Reaction time, ms	183.9 ± 60.6	204.6 ± 91.1	243.1 ± 95.1
Accuracy, %	–	–	–

Accuracy % is the accuracy percentage per trial.



HOA had lower reaction times compared to WMH (congruent:  $P = 0.02$ ; incongruent:  $P = 0.005$ ). Accuracy did not differ between groups (congruent:  $F = 2.3$ ,  $df = 2,64$ ,  $P = 0.1$ ; incongruent:  $F = 0.4$ ,  $df = 2,64$ ,  $P = 0.7$ ). *Executive* contrast of *incongruent* minus *congruent* reaction times did not differ between groups ( $F = 2.3$ ,  $df = 2,64$ ,  $P = 0.1$ ).

## All Versus Baseline Condition Weighted-Echoes fMRI Group Activation Differences

The *all versus baseline* condition activation maps, adjusted for correct-trial reaction time, revealed a network of activation in frontal, subcortical, parietal, and occipital regions (Figure 3 shows the mean activation per group). The HOA group had a greater spatial extent of activation compared to the other groups (Figure 3). Further, group differences in peak activation were observed (omnibus ANOVA:  $P < 0.05$ ). In pairwise comparisons, the HOA group had greater activation than HYA in the occipital lobe, inferior temporal gyrus, middle temporal gyrus, and angular gyrus (Table 3 and Figure 4A). The HOA group also had greater activation compared to WMH in a fronto-temporal region comprising the planum temporale, temporal gyrus, frontal pole, parietal lobe, supramarginal, postcentral, precentral, and middle and frontal gyri, as well as a parieto-occipital region comprising the parietal operculum cortex, lateral occipital cortex, and precuneus cortex (Table 3 and Figure 4B). Moreover, pair-wise comparisons showed that the HYA group had greater activation compared to WMH in an occipital region comprising the calcarine cortex, lingual gyrus, and occipital cortex, pole, and fusiform gyrus, as well as a parieto-occipital region comprising the precuneus, and posterior cingulate gyrus, and right cuneal cortex (Table 3 and Figure 4C). No clusters were found for the reverse contrasts, i.e., the WMH group did not have greater activation than either HOA or HYA. Reaction-time-unadjusted *all versus baseline* condition average activation maps for WMH and HOA were comparable to the reaction-time-adjusted results. An HOA versus HYA contrast was absent in the unadjusted analysis.

## Association of Behavior and Weighted-Echoes fMRI Activation

In the HOA group, there was a mild but significant association between mean reaction time of all task conditions (i.e., incongruent and congruent) on BOLD % signal change ( $R^2 = 0.07$ ,  $P = 0.03$  (Figure 5A)). No associations were observed for either the WMH ( $P = 0.5$ ) or HYA ( $P = 0.5$ ) groups. Further, no association between BOLD % signal change and mean reaction time was observed when data was combined from all groups ( $R^2 = 0.01$ ,  $P = 0.2$ ) (Figure 5A). Accuracy did not correlate with BOLD % signal change for any of the groups individually ( $P > 0.08$ ) or in a combined analysis ( $R^2 = 0.02$ ,  $P = 0.1$ ). Similarly, performance did not correlate to BOLD % in the combined sample when separated into *congruent* (mean reaction time:  $P = 0.8$ ; accuracy:  $P = 0.4$ ; Figure 5B) and *incongruent* conditions (mean reaction time:  $P = 0.4$ ; accuracy:  $P = 0.4$ ; Figure 5C).

## Executive Contrast Weighted-Echoes fMRI Group Activation Differences

The *executive* contrast maps, adjusted for correct-trial reaction time, for the HOA group showed mean activation in the frontal pole, superior and middle frontal gyri, paracingulate gyrus,

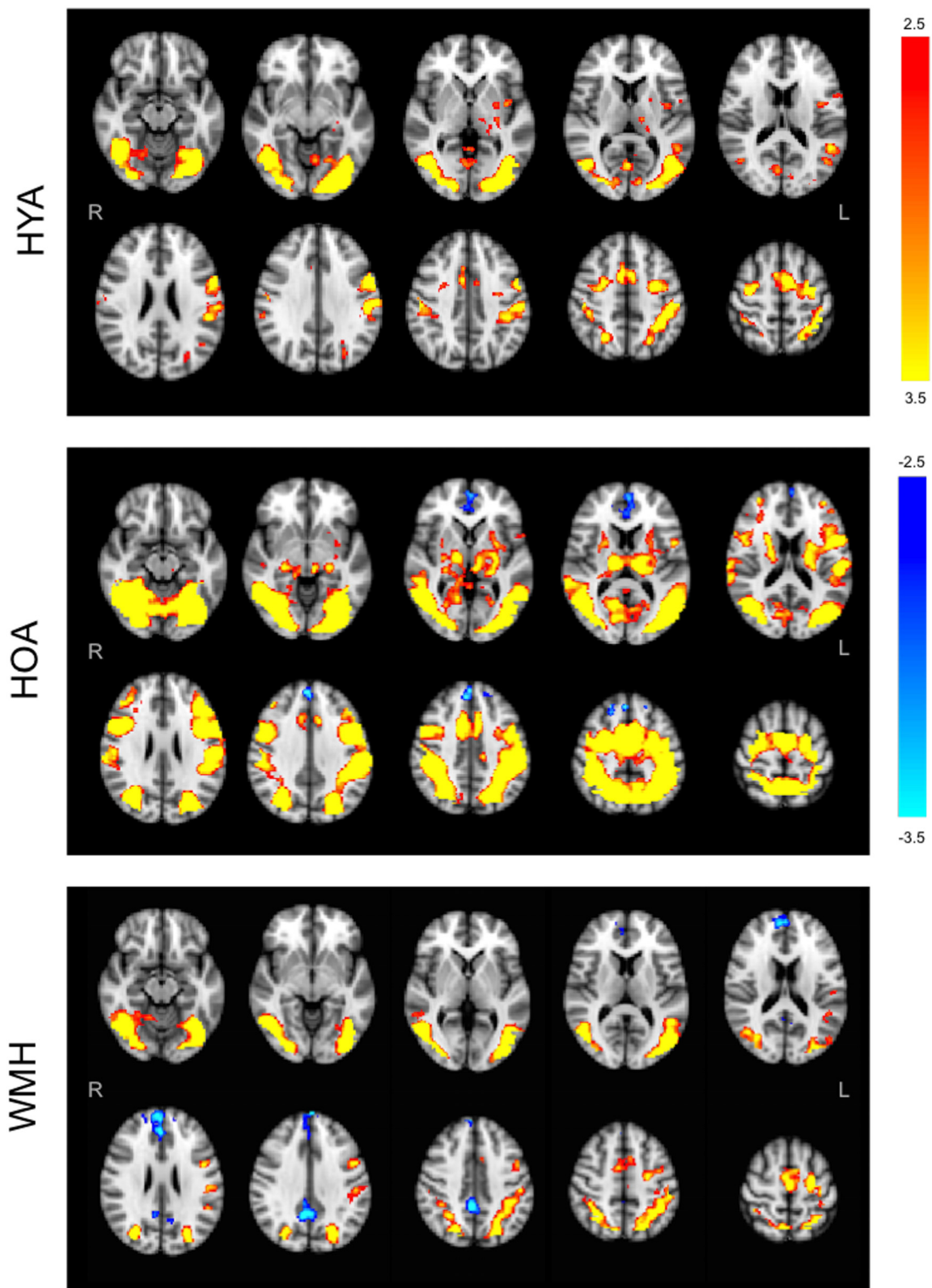


**FIGURE 3** | Group average statistical maps of BOLD fMRI signal for *all versus baseline* condition. HYA activated bilateral sections of the visual and attention networks like the anterior cingulate gyrus, occipital cortex, left insula, parietal opercular, and parietal lobes, and supplementary motor cortex, with no evidence of deactivation. HOA activated the visual and attention networks including fronto-parietal areas, insula, and lateral occipital cortices, with deactivation in the frontal pole, cingulate and paracingulate. WMH demonstrated tightly localized activity in the attention system (middle frontal), with deactivation throughout interoceptive network nodes (frontal regions and precuneus). Primary threshold for all maps was  $Z = 2.32$  and cluster-correction threshold was  $P = 0.05$ . Warm colors, activation relative to fixation. Cool colors, deactivation relative to fixation.

**TABLE 3** | Peak brain activation during all conditions versus baseline and executive contrasts.

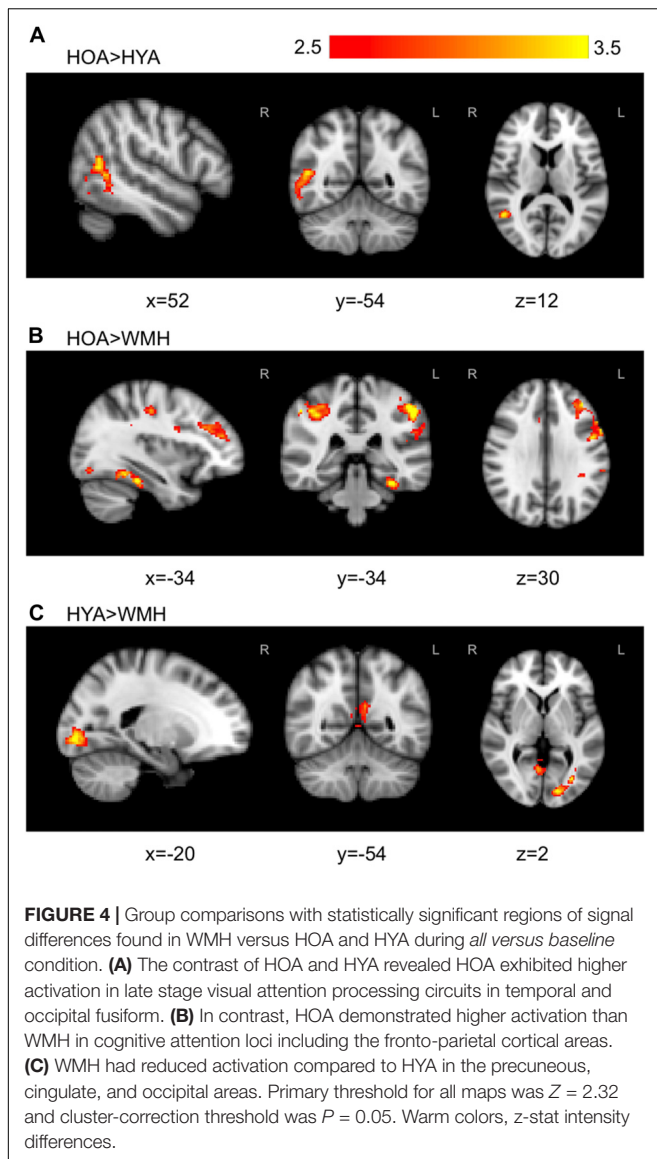
Area	Hemisphere	MNI coordinates			Cluster size (voxels)	Z <sub>peak</sub>
		x	y	z		
<b>All versus baseline condition</b>						
Main effect of HOA (HOA > HYA)						
Temporal occipital fusiform cortex, inferior temporal gyrus, inferior lateral occipital cortex, middle temporal gyrus, angular gyrus.	R	40	-48	-22	569	3.62
Main effect of HOA (HOA > WMH)						
Superior parietal lobule, anterior supramarginal gyrus, postcentral gyrus, precentral gyrus, middle frontal gyrus, inferior frontal gyrus, planum temporale, posterior superior temporal gyrus, frontal pole, parietal operculum cortex.	L	-60	8	28	2064	4.82
R precentral gyrus, R postcentral gyrus, R supramarginal gyrus, L and R superior parietal lobe, R superior lateral occipital cortex, L and R precuneus cortex, R parietal operculum cortex.	L, R	38	-46	54	1609	3.94
Inferior lateral occipital cortex, occipital fusiform gyrus, temporal occipital fusiform cortex, lingual gyrus, inferior temporal gyrus, middle temporal gyrus.	R	40	-50	-22	874	4.09
Occipital pole, inferior lateral occipital cortex, lingual gyrus, posterior temporal fusiform cortex.	L	-6	-96	-4	621	4.93
L and R Paracingulate gyrus, R anterior cingulate gyrus, R middle frontal gyrus, L and R juxtapositional lobule, R precentral gyrus, R superior frontal gyrus.	L,R	28	4	48	613	4.25
Inferior lateral occipital cortex, lingual gyrus, inferior temporal gyrus, posterior temporal fusiform cortex, posterior parahippocampal gyrus, temporal occipital fusiform cortex,	L	-34	-34	-22	542	3.75
Main effect of HYA (HYA > WMH)						
Supracalcarine cortex, intracalcarine cortex, lingual gyrus, inferior lateral occipital cortex, occipital pole, occipital fusiform gyrus.	L	-16	-84	-2	758	3.77
L and R precuneus cortex, L and R lingual gyrus, L and R posterior cingulate gyrus, R cuneal cortex, R supracalcarine cortex.	L, R	6	-62	4	564	3.4
<b>Executive contrast</b>						
Main effect of WMH (WMH > HYA)						
L and R precuneus cortex, R Posterior cingulate gyrus, R cuneal cortex.	L, R	-10	-54	40	767	3.21

Areas defined by the Harvard-Oxford Structural Atlas. L; Left, R; Right, HOA, Healthy Older Adults; WMH, White Matter Hyperintensity group; HYA, Healthy Younger Adults, MNI: Montreal Neurological Institute.

superior parietal lobule, lateral occipital cortex, precuneus, angular gyrus, and supramarginal gyrus. For the WMH group, mean activation was observed in the angular gyrus, superior parietal lobe, precuneus cortex, postcentral gyrus, supramarginal gyrus, lateral occipital cortex, and cingulate gyrus. The HYA group did not show mean activation above threshold for *executive* contrast (data not shown). Group differences were observed in the lateral occipital lobe, superior parietal lobule, supramarginal gyrus, and angular gyrus (omnibus ANOVA:  $P < 0.05$ ). *Post hoc* pairwise group comparison revealed WMH had greater activation compared to HYA in a parieto-occipital region comprising the precuneus, posterior cingulate gyrus, and supracalcarine cortex (Table 3 and Figure 6). No significant clusters were found for the reverse contrast, or any contrast involving the HOA group. Reaction-time-unadjusted *executive* contrasts showed similar average activation patterns in HOA and WMH, and a similar absence of significant voxels for this contrast in HYA. ANOVA did not reveal group differences.

## DISCUSSION

This study implemented multi-echo BOLD fMRI during an attention-demanding test to identify brain activation differences between older adults with and without WMH, as well as young healthy adults. Adults with WMH performed worse on attention-related tasks in terms of processing speed but not accuracy. In concert with our successful efforts of achieving robust fMRI signals through weighted-echo BOLD, the WMH group had a smaller spatial extent of activation patterns compared to HOA, after adjusting for reaction time performance. Notably, individuals with WMH had lower activation in the fronto-parietal regions and temporo-parietal junction compared to HOA. In an *executive* function contrast, WMH activated areas of the precuneus and posterior cingulate gyrus more than HYA, despite similar congruency-related effects on reaction time. These results suggest WMH may contribute to disruption of functional brain networks that underlie salience and cognitively mediated attention.



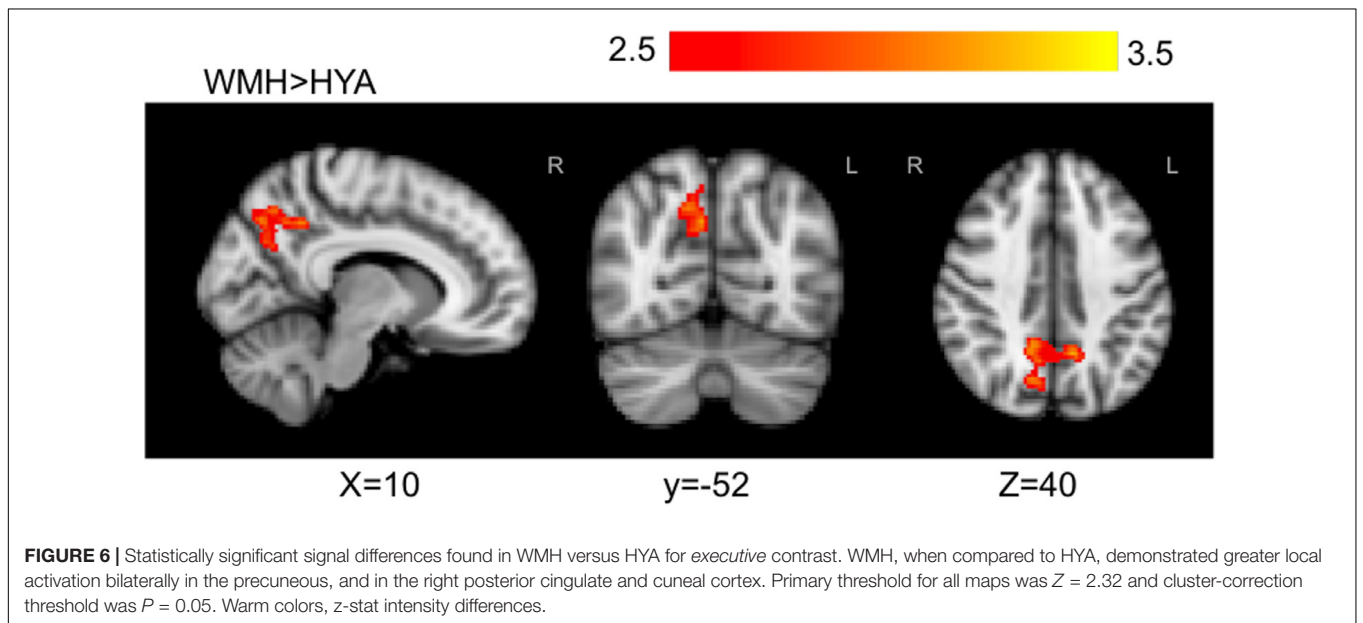
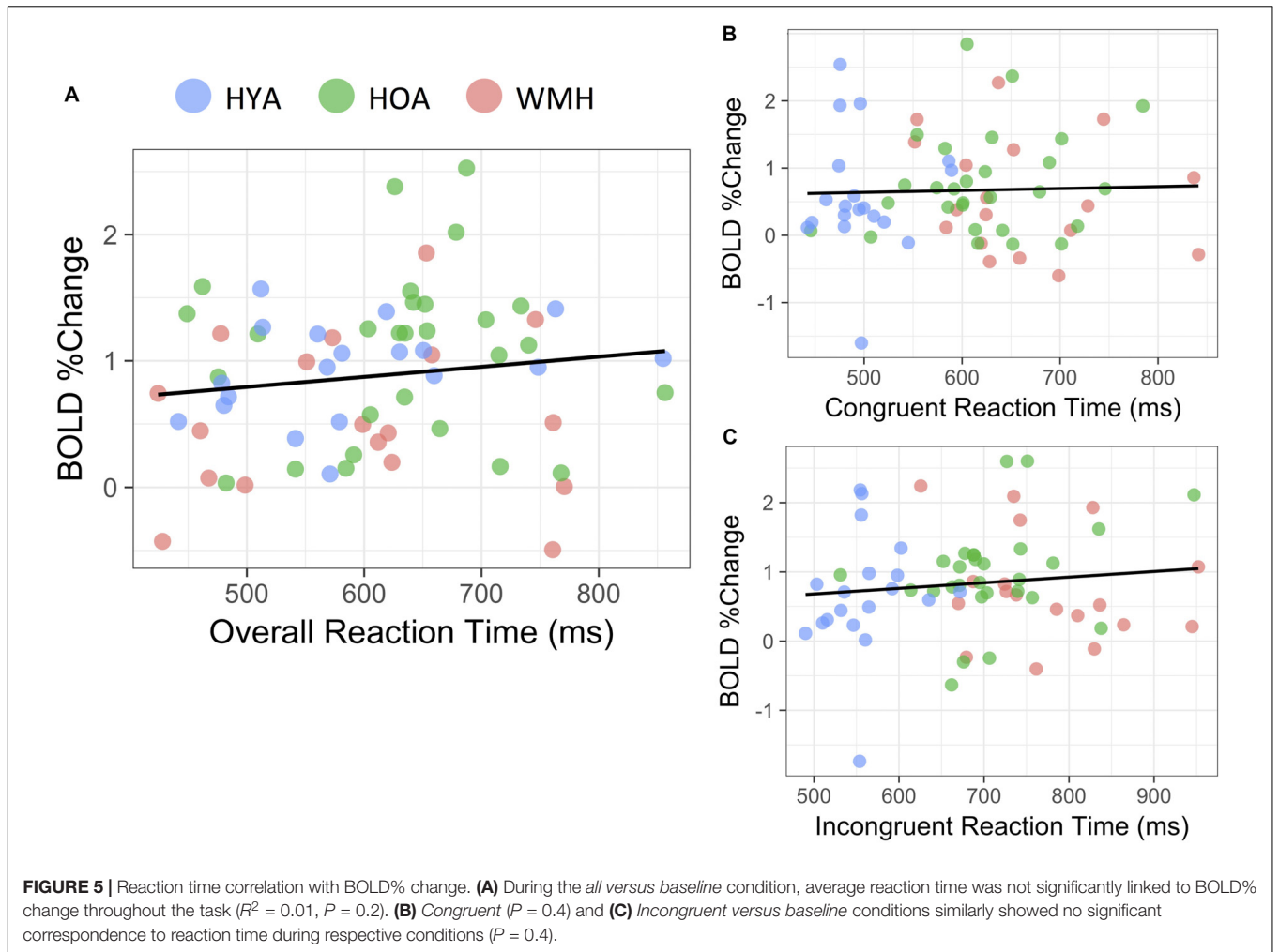
We showed significant group differences using a robust multi-echo BOLD fMRI method, which is an acquisition and analysis strategy that emphasizes activation by diminishing spurious unrelated signal and increasing the contrast to noise ratio (Kundu et al., 2013, 2015, 2017; Gonzalez-Castillo et al., 2016). Recently, researchers have used similar approaches to study fMRI among healthy younger, middle-aged (Kundu et al., 2015; DuPre et al., 2016; Vértes et al., 2016; McDonald et al., 2017), and obese adults (Baek et al., 2017). Our study adds to this body of literature by applying the technique to an older cohort with inherently compromised BOLD signal-to-noise (Huettel et al., 2001). We showed that multi-echo BOLD weighting decreased the global correspondence between the denoised data and the raw data, while maintaining a wider spatial activation compared to RETROICOR (see **Supplementary Figure S1**). A lower slope in WMH using the weighted-echoes method presumably reflects greater removal of physiological and other

noise sources that increase with age and/or disease (Huettel et al., 2001). Further, the effectiveness of RETROICOR was variable across groups, demonstrated by a lower correspondence, that is  $R^2$ , with the single echo fMRI reference in WMH, which may introduce systematic bias to group comparisons of activation. The more nuanced multi-echo BOLD approach differs from RETROICOR's uniform denoising technique and may be beneficial in heterogeneous cohorts where atrophy and/or aging elicit spatially varying influences on BOLD images.

The *all versus baseline* condition is of interest in the current analysis as it highlights total task-positive network activation differences between HOA and WMH that can go undetected in higher-level analyses among older adults. HYA consistently had faster processing speed than HOA without extensive BOLD activation in the current study. In particular, there was greater activation in regions of the occipito-temporal cortex in HOA compared to HYA, a region important for prediction of upcoming motor-action (Gallivan et al., 2013). This may reflect a lower task difficulty for the HYA, which others attribute to down regulation of a task-positive network (Reuter-Lorenz and Cappell, 2008). Increased recruitment of brain resources may be influenced by task difficulty in HOA; a relationship emphasized by elevated activation compared to WMH and HYA and in previous work demonstrating compensatory reallocation during cognitively demanding tasks (Cabeza et al., 2002).

One explanation for the hypoactivation of fronto-parietal and temporal regions seen in WMH, compared to HOA during *all versus baseline* condition, could be that WMH experienced relatively higher cognitive load, which led to hypoactivity within these regions coupled with slower processing speeds. More explicitly, HOA implement a compensation strategy of increased prefrontal and parietal cortex recruitment at low levels of cognitive load compared to younger adults (Mattay et al., 2006; Cappell et al., 2010; Schneider-Garces et al., 2010), however, at higher cognitive load, this strategy often fails and results in equivalent or reduced activity (Grady, 2012; Kennedy et al., 2017). Similar to our findings in WMH, greater WMH lesion volume is associated with lower activation in the left middle frontal gyrus and right posterior parietal cortex (Venkatraman et al., 2010); regions recruited during attentional tasks in healthy older and younger adults (Fan et al., 2002, 2005; Langenecker et al., 2004). The presence of WMH, therefore, may lead to differential neural network responses compared to HOA.

BOLD % signal increased as performance decreased in HOA, but this association was not found in WMH or HYA during the *all versus baseline* condition. This relationship reinforces the link between task performance and cognitive demand in HOA (Cabeza et al., 2002), and highlights a decoupling of performance and neurovascular response in WMH. Our findings are consistent with aspects of neural network theories, in which accumulation of WMH can impact gray matter resting-state/task-based functional connectivity (De Marco et al., 2017) and thus compensatory recruitment (Lockhart et al., 2015; Dey et al., 2016). Indeed, cholinergic fibers are necessary for fronto-parietal, default mode network connections (Cheng et al., 2012) and anterior-posterior coherences (Moretti et al., 2008;



Babiloni et al., 2009). Damage to anterior-posterior tracts that connect dorsolateral prefrontal cortex to the intraparietal sulcus may lead to hypoactivation in WMH (this study, Venkatraman et al., 2010). Loss of inter- and intra-hemispheric connections can interfere with the lateralization and synchronization of network nodes (Marstaller et al., 2015), which in turn can explain poor cognitive performance in WMH. There are limited functional connectivity analyses explicitly in WMH; future studies using resting-state fMRI connectivity would provide important insight into this potential neural network breakdown.

The effect of congruency (i.e., *executive* condition) during the flanker task further characterized the WMH brain network profile. Our findings are consistent with evidence that executive function performance, probed by the attention network test, is equivalent in older and younger adults (Fernandez-Duque and Black, 2006; Jennings et al., 2007). We found no difference in executive contrast activation between older adult groups. The WMH group did not show activation in frontal regions that was observed in HOA (data not shown); this may reflect reduced connectivity in prefrontal regions in WMH as seen from resting-state fMRI (Schaefer et al., 2014). This pattern did not map onto executive behavioral performance, potentially due to the poor association of periventricular WMH with executive function (Prins et al., 2005). This analysis could have been limited by low statistical power, reducing the effect of group activation differences using an active baseline. The WMH group had higher BOLD response compared to HYA during the *executive* contrast, which is consistent with other studies on executive function (Gold et al., 2017) and spatial search tasks (Lockhart et al., 2015; Gold et al., 2017), and is linked with white matter tract deterioration (Madden et al., 2007; Persson et al., 2011). Unlike reports of frontal-network over-activation (Lockhart et al., 2015; Gold et al., 2017), WMH atypically recruited highly vascularized areas of the precuneus and posterior cingulate. The precuneus, posterior cingulate cortex, and surrounding regions are a core feature of the default mode network (McKiernan et al., 2003). However, the posterior cingulate-precuneus network exhibits hyper-activation during task in attention-deficit/hyperactivity disorder (Castellanos et al., 2008), and evidence points to its recruitment under specific task-positive conditions (Utevsky et al., 2014). Underlying differences in neural activation of these areas in WMH are more likely explained by impaired physiology such as vascular deterioration and subsequent hypoperfusion (Miners et al., 2016), and/or reduced glucose metabolism (Hirono et al., 2004; Choo et al., 2007; Brown et al., 2014; Miners et al., 2016).

The limitations of this study are as follows. Group differences in the *all versus baseline* fMRI signal may be influenced by alterations in the hemodynamic response, which is described in overt stroke groups but has yet to be investigated among adults with subclinical WMH (Roc et al., 2006; Blicher et al., 2012). A delayed hemodynamic response is plausible given the pathophysiological features of WMH, namely endothelial dysfunction, atherosclerosis and arteriosclerosis (Wardlaw et al., 2013). Moreover, the need to identify WMH presence *a priori*, which we addressed by pre-study screening for vascular risk

factors, through a family medicine clinic mail-out, limited recruitment efforts. The current study does not separate individuals by other forms of small vessel disease such as cerebral microbleeds or enlarged perivascular spaces. Considering the Fazekas scoring system is widely used, there is clinical prudence to separating the cohorts based on this rating scheme. The current study investigated fMRI activation differences from one attention-related task, which was chosen due to attention and psychomotor speed as hallmark cognitive features of WMH; however, future studies exploiting multi-domain cognitive fMRI may provide added insight. Finally, we acknowledge that recent debates highlighting potentially high false-positive rates in fMRI studies might have bearing on single-echo BOLD data (Eklund et al., 2016; Slotnick, 2017). Methods comparison analysis in this study shows reduced signal compared to single-echo data used in such conventional fMRI studies, therefore, we in part used weighted multi-echo data to account for potentially inflated false positive rates (Lombardo et al., 2016).

## CONCLUSION

This study identified a dichotomy between older adults with and without WMH, characterized by brain activation differences elicited by an attention network task during multi-echo fMRI. We observed weak brain-behavior links, which subsequently fail to elucidate how neural network strategies may be applied to performance. This sets the precedent for exploring WMH-linked network dysfunction through resting-state fMRI analyses. Subsequent studies should also explore the nature of the blood-tissue transfer of oxygen in those with neurovascular pathology to further our understanding of the neurophysiological consequences of CSVD.

## AUTHOR CONTRIBUTIONS

SA, AM, and BM conceived and designed the research. SA performed the experiments and analyzed the data. SA and BM interpreted results of experiments. SA prepared the figures and drafted the manuscript. SA and BM edited and revised the manuscript. All authors provided feedback on manuscript. SA and BM approved final version of the manuscript.

## FUNDING

This work was supported by the Canadian Institute of Health Research (Grant Nos. MOP133568 and 2014); Canadian Consortium on Neurodegeneration in Ageing (2014); and the Alzheimer's Society of Canada (2015).

## SUPPLEMENTARY MATERIAL

The Supplementary Material for this article can be found online at: <https://www.frontiersin.org/articles/10.3389/fnins.2018.00748/full#supplementary-material>

## REFERENCES

- Andersson, J. L. R., Jenkinson, M., Smith, S., and Others (2007). *Non-Linear Registration, Aka Spatial Normalisation FMRIB Technical Report TR07JA2. FMRIB Analysis Group of the University of Oxford 2*. Available at: <https://www.fmrib.ox.ac.uk/datasets/techrep/tr07ja2/tr07ja2.pdf>
- Babiloni, C., Pievani, M., Vecchio, F., Geroldi, C., Eusebi, F., Fracassi, C., et al. (2009). White-matter lesions along the cholinergic tracts are related to cortical sources of EEG rhythms in amnesic mild cognitive impairment. *Hum. Brain Mapp.* 30, 1431–1443. doi: 10.1002/hbm.20612
- Baek, K., Morris, L. S., Kundu, P., and Voon, V. (2017). Disrupted resting-state brain network properties in obesity: decreased global and putaminal cortico-striatal network efficiency. *Psychol. Med.* 47, 585–596. doi: 10.1017/S0033291716002646
- Barnes, J., Carmichael, O. T., Leung, K. K., Schwarz, C., Ridgway, G. R., Bartlett, J. W., et al. (2013). Vascular and Alzheimer's disease markers independently predict brain atrophy rate in Alzheimer's disease neuroimaging initiative controls. *Neurobiol. Aging* 34, 1996–2002. doi: 10.1016/j.neurobiolaging.2013.02.003
- Bastos-Leite, A. J., Kuijter, J. P. A., Rombouts, S. A. R. B., Sanz-Arigitia, E., van Straaten, E. C., Gouw, A. A., et al. (2008). Cerebral blood flow by using pulsed arterial spin-labeling in elderly subjects with white matter hyperintensities. *AJNR Am. J. Neuroradiol.* 29, 1296–1301. doi: 10.3174/ajnr.A1091
- Beckmann, C. F., Jenkinson, M., and Smith, S. M. (2003). General multilevel linear modeling for group analysis in fMRI. *Neuroimage* 20, 1052–1063. doi: 10.1016/S1053-8119(03)00435-X
- Birn, R. M., Diamond, J. B., Smith, M. A., and Bandettini, P. A. (2006). Separating respiratory-variation-related fluctuations from neuronal-activity-related fluctuations in fMRI. *Neuroimage* 31, 1536–1548. doi: 10.1016/j.neuroimage.2006.02.048
- Biswal, B., Deyoe, E. A., and Hyde, J. S. (1996). Reduction of physiological fluctuations in fMRI using digital filters. *Magn. Reson. Med.* 35, 107–113. doi: 10.1002/mrm.1910350114
- Blicher, J. U., Stagg, C. J., O'Shea, J., Østergaard, L., MacIntosh, B. J., Johansen-Berg, H., et al. (2012). Visualization of altered neurovascular coupling in chronic stroke patients using multimodal functional MRI. *J. Cereb. Blood Flow Metab.* 32, 2044–2054. doi: 10.1038/jcbfm.2012.105
- Breteler, M. M., van Amerongen, N. M., van Swieten, J. C., Claus, J. J., Grobbee, D. E., van Gijn, J., et al. (1994). Cognitive correlates of ventricular enlargement and cerebral white matter lesions on magnetic resonance imaging, rotterdam study. *Stroke* 25, 1109–1115. doi: 10.1161/01.STR.25.6.1109
- Brown, R. K. J., Bohnen, N. I., Wong, K. K., Minoshima, S., and Frey, K. A. (2014). Brain PET in suspected dementia: patterns of altered FDG metabolism. *Radiographics* 34, 684–701. doi: 10.1148/rg.343135065
- Buur, P. F., Norris, D. G., and Hesse, C. W. (2008). Extraction of task-related activation from multi-echo BOLD fMRI. *IEEE J. Sel. Top. Signal Process.* 2, 954–964. doi: 10.1109/JSTSP.2008.2007817
- Buur, P. F., Poser, B. A., and Norris, D. G. (2009). A dual echo approach to removing motion artefacts in fMRI time series. *NMR Biomed.* 22, 551–560. doi: 10.1002/nbm.1371
- Caballero-Gaudes, C., and Reynolds, R. C. (2016). Methods for cleaning the BOLD fMRI signal. *Neuroimage* 154, 128–149. doi: 10.1016/j.neuroimage.2016.12.018
- Cabeza, R., Anderson, N. D., Locantore, J. K., and McIntosh, A. R. (2002). Aging gracefully: compensatory brain activity in high-performing older adults. *Neuroimage* 17, 1394–1402. doi: 10.1006/nimg.2002.1280
- Cappell, K. A., Gmeindl, L., and Reuter-Lorenz, P. A. (2010). Age differences in prefrontal recruitment during verbal working memory maintenance depend on memory load. *Cortex* 46, 462–473. doi: 10.1016/j.cortex.2009.11.009
- Castellanos, F. X., Margulies, D. S., Kelly, C., Uddin, L. Q., Ghaffari, M., Kirsch, A., et al. (2008). Cingulate-precuneus interactions: a new locus of dysfunction in adult attention-deficit/hyperactivity disorder. *Biol. Psychiatry* 63, 332–337. doi: 10.1016/j.biopsych.2007.06.025
- Cheng, H.-L., Lin, C.-J., Soong, B.-W., Wang, P.-N., Chang, F.-C., Wu, Y.-T., et al. (2012). Impairments in cognitive function and brain connectivity in severe asymptomatic carotid stenosis. *Stroke* 43, 2567–2573. doi: 10.1161/STROKEAHA.111.645614
- Choo, I. H., Lee, D. Y., Youn, J. C., Jhoo, J. H., Kim, K. W., Lee, D. S., et al. (2007). Topographic patterns of brain functional impairment progression according to clinical severity staging in 116 Alzheimer disease patients: FDG-PET study. *Alzheimer Dis. Assoc. Disord.* 21, 77–84. doi: 10.1097/WAD.0b013e3180687418
- de Groot, J. C., de Leeuw, F. E., Oudkerk, M., van Gijn, J., Hofman, A., Jolles, J., et al. (2000). Cerebral white matter lesions and cognitive function: the Rotterdam Scan Study. *Ann. Neurol.* 47, 145–151. doi: 10.1002/1531-8249(200002)47:2<145::AID-ANA3>3.0.CO;2-P
- De Marco, M., Manca, R., Mitolo, M., and Venneri, A. (2017). White matter hyperintensity load modulates brain morphometry and brain connectivity in healthy adults: a neuroplastic mechanism? *Neural Plast.* 2017:4050536. doi: 10.1155/2017/4050536
- Dey, A. K., Stamenova, V., Turner, G., Black, S. E., and Levine, B. (2016). Pathoconnectomics of cognitive impairment in small vessel disease: a systematic review. *Alzheimers Dement.* 12, 831–845. doi: 10.1016/j.jalz.2016.01.007
- DuPre, E., Luh, W.-M., and Spreng, R. N. (2016). Multi-echo fMRI replication sample of autobiographical memory, prospection and theory of mind reasoning tasks. *Sci. Data* 3:160116. doi: 10.1038/sdata.2016.116
- Eklund, A., Nichols, T. E., and Knutsson, H. (2016). Cluster failure: why fMRI inferences for spatial extent have inflated false-positive rates. *Proc. Natl. Acad. Sci. U.S.A.* 113, 7900–7905. doi: 10.1073/pnas.1602413113
- Fan, J., McCandliss, B. D., Fossella, J., Flombaum, J. I., and Posner, M. I. (2005). The activation of attentional networks. *Neuroimage* 26, 471–479. doi: 10.1016/j.neuroimage.2005.02.004
- Fan, J., McCandliss, B. D., Sommer, T., Raz, A., and Posner, M. I. (2002). Testing the efficiency and independence of attentional networks. *J. Cogn. Neurosci.* 14, 340–347. doi: 10.1162/089982902317361886
- Fazekas, F., Barkhof, F., Wahlund, L. O., Pantoni, L., Erkinjuntti, T., Scheltens, P., et al. (2002). CT and MRI rating of white matter lesions. *Cerebrovasc. Dis.* 13(Suppl. 2), 31–36. doi: 10.1159/000049147
- Fernandez-Duque, D., and Black, S. E. (2006). Attentional networks in normal aging and Alzheimer's disease. *Neuropsychology* 20, 133–143. doi: 10.1037/0894-4105.20.2.133
- Fu, J., Tang, J., Han, J., and Hong, Z. (2014). The reduction of regional cerebral blood flow in normal-appearing white matter is associated with the severity of white matter lesions in elderly: a Xeon-CT study. *PLoS One* 9:e112832. doi: 10.1371/journal.pone.0112832
- Gallivan, J. P., Chapman, C. S., McLean, D. A., Flanagan, J. R., and Culham, J. C. (2013). Activity patterns in the category-selective occipitotemporal cortex predict upcoming motor actions. *Eur. J. Neurosci.* 38, 2408–2424. doi: 10.1111/ejn.12215
- Gibson, E., Gao, F., Black, S. E., and Lobaugh, N. J. (2010). Automatic segmentation of white matter hyperintensities in the elderly using FLAIR images at 3T. *J. Magn. Reson. Imaging* 31, 1311–1322. doi: 10.1002/jmri.22004
- Glover, G. H., Li, T., and Ress, D. (2000). Image-based method for retrospective correction of physiological motion effects in fMRI: RETROICOR. *Magn. Reson. Med.* 44, 162–167. doi: 10.1002/1522-2594(200007)44:1<162::AID-MRM23>3.0.CO;2-E
- Gold, B. T., Brown, C. A., Hakun, J. G., Shaw, L. M., Trojanowski, J. Q., and Smith, C. D. (2017). Clinically silent Alzheimer's and vascular pathologies influence brain networks supporting executive function in healthy older adults. *Neurobiol. Aging* 58, 102–111. doi: 10.1016/j.neurobiolaging.2017.06.012
- Gonzalez-Castillo, J., Panwar, P., Buchanan, L. C., Caballero-Gaudes, C., Handwerker, D. A., Jangraw, D. C., et al. (2016). Evaluation of multi-echo ICA denoising for task based fMRI studies: block designs, rapid event-related designs, and cardiac-gated fMRI. *Neuroimage* 141, 452–468. doi: 10.1016/j.neuroimage.2016.07.049
- Grady, C. (2012). The cognitive neuroscience of ageing. *Nat. Rev. Neurosci.* 13, 491–505. doi: 10.1038/nrn3256
- Greve, D. N., and Fischl, B. (2009). Accurate and robust brain image alignment using boundary-based registration. *Neuroimage* 48, 63–72. doi: 10.1016/j.neuroimage.2009.06.060
- Hedden, T., Van Dijk, K. R. A., Shire, E. H., Sperling, R. A., Johnson, K. A., and Buckner, R. L. (2012). Failure to modulate attentional control in advanced aging linked to white matter pathology. *Cereb. Cortex* 22, 1038–1051. doi: 10.1093/cercor/bhr172
- Hirono, N., Hashimoto, M., Ishii, K., Kazui, H., and Mori, E. (2004). One-year change in cerebral glucose metabolism in patients with Alzheimer's

- disease. *J. Neuropsychiatry Clin. Neurosci.* 16, 488–492. doi: 10.1176/jnp.16.4.488
- Hu, X., Le, T. H., Parrish, T., and Erhard, P. (1995). Retrospective estimation and correction of physiological fluctuation in functional MRI. *Magn. Reson. Med.* 34, 201–212. doi: 10.1002/mrm.1910340211
- Huettel, S. A., Singerman, J. D., and McCarthy, G. (2001). The effects of aging upon the hemodynamic response measured by functional MRI. *Neuroimage* 13, 161–175. doi: 10.1006/nimg.2000.0675
- Ishikawa, H., Meguro, K., Ishii, H., Tanaka, N., and Yamaguchi, S. (2012). Silent infarction or white matter hyperintensity and impaired attention task scores in a nondemented population: the Osaka-Tajiri Project. *J. Stroke Cerebrovasc. Dis.* 21, 275–282. doi: 10.1016/j.jstrokecerebrovasdis.2010.08.008
- Jenkinson, M., Bannister, P., Brady, M., and Smith, S. (2002). Improved optimization for the robust and accurate linear registration and motion correction of brain images. *Neuroimage* 17, 825–841. doi: 10.1006/nimg.2002.1132
- Jenkinson, M., and Smith, S. (2001). A global optimisation method for robust affine registration of brain images. *Med. Image Anal.* 5, 143–156. doi: 10.1016/S1361-8415(01)00036-6
- Jennings, J. M., Dagenbach, D., Engle, C. M., and Funke, L. J. (2007). Age-related changes and the attention network task: an examination of alerting, orienting, and executive function. *Neuropsychol. Dev. Cogn. B Aging Neuropsychol. Cogn.* 14, 353–369. doi: 10.1080/13825580600788837
- Kennedy, K. M., Rieck, J. R., Boylan, M. A., and Rodrigue, K. M. (2017). Functional magnetic resonance imaging data of incremental increases in visuo-spatial difficulty in an adult lifespan sample. *Data Brief* 11, 54–60. doi: 10.1016/j.dib.2017.01.004
- Kerchner, G. A., Racine, C. A., Hale, S., Wilhelm, R., Laluz, V., Miller, B. L., et al. (2012). Cognitive processing speed in older adults: relationship with white matter integrity. *PLoS One* 7:e50425. doi: 10.1371/journal.pone.0050425
- Kirilina, E., Lutti, A., Poser, B. A., Blankenburg, F., and Weiskopf, N. (2016). The quest for the best: the impact of different EPI sequences on the sensitivity of random effect fMRI group analyses. *Neuroimage* 126, 49–59. doi: 10.1016/j.neuroimage.2015.10.071
- Kundu, P., Benson, B. E., Baldwin, K. L., Rosen, D., Luh, W.-M., Bandettini, P. A., et al. (2015). Robust resting state fMRI processing for studies on typical brain development based on multi-echo EPI acquisition. *Brain Imaging Behav.* 9, 56–73. doi: 10.1007/s11682-014-9346-4
- Kundu, P., Brenowitz, N. D., Voon, V., Worbe, Y., Vértes, P. E., Inati, S. J., et al. (2013). Integrated strategy for improving functional connectivity mapping using multiecho fMRI. *Proc. Natl. Acad. Sci. U.S.A.* 110, 16187–16192. doi: 10.1073/pnas.1301725110
- Kundu, P., Voon, V., Balchandani, P., Lombardo, M. V., Poser, B. A., and Bandettini, P. A. (2017). Multi-echo fMRI: a review of applications in fMRI denoising and analysis of BOLD signals. *Neuroimage* 154, 59–80. doi: 10.1016/j.neuroimage.2017.03.033
- Langenecker, S. A., Nielson, K. A., and Rao, S. M. (2004). fMRI of healthy older adults during Stroop interference. *Neuroimage* 21, 192–200. doi: 10.1016/j.neuroimage.2003.08.027
- Lockhart, S. N., Luck, S. J., Geng, J., Beckett, L., Disbrow, E. A., Carmichael, O., et al. (2015). White matter hyperintensities among older adults are associated with futile increase in frontal activation and functional connectivity during spatial search. *PLoS One* 10:e0122445. doi: 10.1371/journal.pone.0122445
- Lombardo, M. V., Auyeung, B., Holt, R. J., Waldman, J., Ruigrok, A. N. V., Mooney, N., et al. (2016). Improving effect size estimation and statistical power with multi-echo fMRI and its impact on understanding the neural systems supporting mentalizing. *Neuroimage* 142, 55–66. doi: 10.1016/j.neuroimage.2016.07.022
- Madden, D. J., Spaniol, J., Whiting, W. L., Bucur, B., Provenzale, J. M., Cabeza, R., et al. (2007). Adult age differences in the functional neuroanatomy of visual attention: a combined fMRI and DTI study. *Neurobiol. Aging* 28, 459–476. doi: 10.1016/j.neurobiolaging.2006.01.005
- Makedonov, I., Black, S. E., and MacIntosh, B. J. (2013). Cerebral small vessel disease in aging and Alzheimer's disease: a comparative study using MRI and SPECT. *Eur. J. Neurol.* 20, 243–250. doi: 10.1111/j.1468-1331.2012.03785.x
- Marstaller, L., Williams, M., Rich, A., Savage, G., and Burianová, H. (2015). Aging and large-scale functional networks: white matter integrity, gray matter volume, and functional connectivity in the resting state. *Neuroscience* 290, 369–378. doi: 10.1016/j.neuroscience.2015.01.049
- Mattay, V. S., Fera, F., Tessitore, A., Hariri, A. R., Berman, K. F., Das, S., et al. (2006). Neurophysiological correlates of age-related changes in working memory capacity. *Neurosci. Lett.* 392, 32–37. doi: 10.1016/j.neulet.2005.09.025
- McDonald, A. R., Muraskin, J., Dam, N. T. V., Froehlich, C., Puccio, B., Pellman, J., et al. (2017). The real-time fMRI neurofeedback based stratification of Default Network Regulation Neuroimaging data repository. *Neuroimage* 146, 157–170. doi: 10.1016/j.neuroimage.2016.10.048
- McKiernan, K. A., Kaufman, J. N., Kucera-Thompson, J., and Binder, J. R. (2003). A parametric manipulation of factors affecting task-induced deactivation in functional neuroimaging. *J. Cogn. Neurosci.* 15, 394–408. doi: 10.1162/089892903321593117
- Miners, J. S., Palmer, J. C., and Love, S. (2016). Pathophysiology of hypoperfusion of the precuneus in early Alzheimer's disease. *Brain Pathol.* 26, 533–541. doi: 10.1111/bpa.12331
- Moretti, D. V., Frisoni, G. B., Pievani, M., Rosini, S., Geroldi, C., Binetti, G., et al. (2008). Cerebrovascular disease and hippocampal atrophy are differentially linked to functional coupling of brain areas: an EEG coherence study in MCI subjects. *J. Alzheimers Dis.* 14, 285–299. doi: 10.3233/JAD-2008-14303
- Nordahl, C. W., Ranganath, C., Yonelinas, A. P., Decarli, C., Fletcher, E., and Jagust, W. J. (2006). White matter changes compromise prefrontal cortex function in healthy elderly individuals. *J. Cogn. Neurosci.* 18, 418–429. doi: 10.1162/jocn.2006.18.3.418
- Olafsson, V., Kundu, P., Wong, E. C., Bandettini, P. A., and Liu, T. T. (2015). Enhanced identification of BOLD-like components with multi-echo simultaneous multi-slice (MESMS) fMRI and multi-echo ICA. *Neuroimage* 112, 43–51. doi: 10.1016/j.neuroimage.2015.02.052
- O'Sullivan, M., Lythgoe, D. J., Pereira, A. C., Summers, P. E., Jarosz, J. M., Williams, S. C. R., et al. (2002). Patterns of cerebral blood flow reduction in patients with ischemic leukoaraiosis. *Neurology* 59, 321–326. doi: 10.1212/WNL.59.3.321
- Pantoni, L. (2010). Cerebral small vessel disease: from pathogenesis and clinical characteristics to therapeutic challenges. *Lancet Neurol.* 9, 689–701. doi: 10.1016/S1474-4422(10)70104-6
- Persson, J., Kalpouzos, G., Nilsson, L.-G., Ryberg, M., and Nyberg, L. (2011). Preserved hippocampus activation in normal aging as revealed by fMRI. *Hippocampus* 21, 753–766. doi: 10.1002/hipo.20794
- Poser, B. A., Versluis, M. J., Hoogduin, J. M., and Norris, D. G. (2006). BOLD contrast sensitivity enhancement and artifact reduction with multiecho EPI: parallel-acquired inhomogeneity-desensitized fMRI. *Magn. Reson. Med.* 55, 1227–1235. doi: 10.1002/mrm.20900
- Posse, S., Wiese, S., Gembris, D., Mathiak, K., Kessler, C., Grosse-Ruyken, M. L., et al. (1999). Enhancement of BOLD-contrast sensitivity by single-shot multi-echo functional MR imaging. *Magn. Reson. Med.* 42, 87–97. doi: 10.1002/(SICI)1522-2594(199907)42:1<87::AID-MRM13>3.0.CO;2-O
- Prins, N. D., van Dijk, E. J., den Heijer, T., Vermeer, S. E., Jolles, J., Koudstaal, P. J., et al. (2005). Cerebral small-vessel disease and decline in information processing speed, executive function and memory. *Brain* 128, 2034–2041. doi: 10.1093/brain/awh553
- Reuter-Lorenz, P. A., and Cappell, K. A. (2008). Neurocognitive aging and the compensation hypothesis. *Curr. Dir. Psychol. Sci.* 17, 177–182. doi: 10.1111/j.1467-8721.2008.00570.x
- Roc, A. C., Wang, J., Ances, B. M., Liebeskind, D. S., Kasner, S. E., and Detre, J. A. (2006). Altered hemodynamics and regional cerebral blood flow in patients with hemodynamically significant stenoses. *Stroke* 37, 382–387. doi: 10.1161/01.STR.0000198807.31299.43
- Rost, N. S., Rahman, R. M., Biffi, A., Smith, E. E., Kanakis, A., Fitzpatrick, K., et al. (2010). White matter hyperintensity volume is increased in small vessel stroke subtypes. *Neurology* 75, 1670–1677. doi: 10.1212/WNL.0b013e3181fc279a
- Schaefer, A., Quinque, E. M., Kipping, J. A., Arélin, K., Roggenhofer, E., Frisch, S., et al. (2014). Early small vessel disease affects frontoparietal and cerebellar hubs in close correlation with clinical symptoms—A resting-state fMRI study. *J. Cereb. Blood Flow Metab.* 34, 1091–1095. doi: 10.1038/jcbfm.2014.70
- Schmidt, W.-P., Roesler, A., Kretschmar, K., Ladwig, K.-H., Junker, R., and Berger, K. (2004). Functional and cognitive consequences of silent stroke discovered using brain magnetic resonance imaging in an elderly population. *J. Am. Geriatr. Soc.* 52, 1045–1050. doi: 10.1111/j.1532-5415.2004.52300.x

- Schneider-Garces, N. J., Gordon, B. A., Brumback-Peltz, C. R., Shin, E., Lee, Y., Sutton, B. P., et al. (2010). Span, CRUNCH, and beyond: working memory capacity and the aging brain. *J. Cogn. Neurosci.* 22, 655–669. doi: 10.1162/jocn.2009.21230
- Shi, Y., Thrippleton, M. J., Makin, S. D., Marshall, I., Geerlings, M. I., de Craen, A. J., et al. (2016). Cerebral blood flow in small vessel disease: a systematic review and meta-analysis. *J. Cereb. Blood Flow Metab.* 36, 1653–1667. doi: 10.1177/0271678X16662891
- Slotnick, S. D. (2017). Cluster success: fMRI inferences for spatial extent have acceptable false-positive rates. *Cogn. Neurosci.* 8, 150–155. doi: 10.1080/17588928.2017.1319350
- Smith, S. M. (2002). Fast robust automated brain extraction. *Hum. Brain Mapp.* 17, 143–155. doi: 10.1002/hbm.10062
- Snowdon, D. A., Greiner, L. H., Mortimer, J. A., Riley, K. P., Greiner, P. A., and Markesbery, W. R. (1997). Brain infarction and the clinical expression of Alzheimer disease: the nun study. *JAMA* 277, 813–817. doi: 10.1001/jama.1997.03540340047031
- Spreng, R. N., Sepulcre, J., Turner, G. R., Stevens, W. D., and Schacter, D. L. (2013). Intrinsic architecture underlying the relations among the default, dorsal attention, and frontoparietal control networks of the human brain. *J. Cogn. Neurosci.* 25, 74–86. doi: 10.1162/jocn\_a\_00281
- Utevsky, A. V., Smith, D. V., and Huettel, S. A. (2014). Precuneus is a functional core of the default-mode network. *J. Neurosci.* 34, 932–940. doi: 10.1523/JNEUROSCI.4227-13.2014
- Venkatraman, V. K., Aizenstein, H., Guralnik, J., Newman, A. B., Glynn, N. W., Taylor, C., et al. (2010). Corrigendum to “Executive control function, brain activation and white matter hyperintensities in older adults” [NeuroImage 49 (2010) 3436–3442]. *Neuroimage* 50:1711. doi: 10.1016/j.neuroimage.2010.01.074
- Vermeer, S. E., Hollander, M., van Dijk, E. J., Hofman, A., Koudstaal, P. J., Breteler, M. M. B., et al. (2003). Silent brain infarcts and white matter lesions increase stroke risk in the general population: the rotterdam scan study. *Stroke* 34, 1126–1129. doi: 10.1161/01.STR.0000068408.82115.D2
- Vértes, P. E., Rittman, T., Whitaker, K. J., Romero-Garcia, R., Váša, F., Kitzbichler, M. G., et al. (2016). Gene transcription profiles associated with inter-modular hubs and connection distance in human functional magnetic resonance imaging networks. *Philos. Trans. R. Soc. Lond. B Biol. Sci.* 371. doi: 10.1098/rstb.2015.0362
- Wagner, M., Helfrich, M., Volz, S., Magerkurth, J., Blasel, S., Porto, L., et al. (2015). Quantitative T2, T2\*, and T2' MR imaging in patients with ischemic leukoaraiosis might detect microstructural changes and cortical hypoxia. *Neuroradiology* 57, 1023–1030. doi: 10.1007/s00234-015-1565-x
- Wardlaw, J. M., Smith, C., and Dichgans, M. (2013). Mechanisms of sporadic cerebral small vessel disease: insights from neuroimaging. *Lancet Neurol.* 12, 483–497. doi: 10.1016/S1474-4422(13)70060-7
- Witt, S. T., Warntjes, M., and Engström, M. (2016). Increased fMRI sensitivity at equal data burden using averaged shifted echo acquisition. *Front. Neurosci.* 10:544. doi: 10.3389/fnins.2016.00544
- Woolrich, M. W., Behrens, T. E. J., Beckmann, C. F., Jenkinson, M., and Smith, S. M. (2004). Multilevel linear modelling for FMRI group analysis using Bayesian inference. *Neuroimage* 21, 1732–1747. doi: 10.1016/j.neuroimage.2003.12.023
- Wowk, B., McIntyre, M. C., and Saunders, J. K. (1997). k-Space detection and correction of physiological artifacts in fMRI. *Magn. Reson. Med.* 38, 1029–1034. doi: 10.1002/mrm.1910380625
- Wright, C. B., Festa, J. R., Paik, M. C., Schmiedigen, A., Brown, T. R., Yoshita, M., et al. (2008). White matter hyperintensities and subclinical infarction: associations with psychomotor speed and cognitive flexibility. *Stroke* 39, 800–805. doi: 10.1161/STROKEAHA.107.484147
- Zhang, Y., Brady, M., and Smith, S. (2001). Segmentation of brain MR images through a hidden Markov random field model and the expectation-maximization algorithm. *IEEE Trans. Med. Imaging* 20, 45–57. doi: 10.1109/42.906424
- Zheng, J. J. J., Lord, S. R., Close, J. C. T., Sachdev, P. S., Wen, W., Brodaty, H., et al. (2012). Brain white matter hyperintensities, executive dysfunction, instability, and falls in older people: a prospective cohort study. *J. Gerontol. A Biol. Sci. Med. Sci.* 67, 1085–1091. doi: 10.1093/gerona/gls063
- Zheng, L. S., Xu, J., and Wang, J. P. (2006). Quantitative evaluation of regional cerebral blood flow in patients with silent Leukoaraiosis. *Chin. J. Clin. Rehabil.* 10, 80–82.

**Conflict of Interest Statement:** The authors declare that the research was conducted in the absence of any commercial or financial relationships that could be construed as a potential conflict of interest.

Copyright © 2018 Atwi, Metcalfe, Robertson, Rezmovitz, Anderson and MacIntosh. This is an open-access article distributed under the terms of the Creative Commons Attribution License (CC BY). The use, distribution or reproduction in other forums is permitted, provided the original author(s) and the copyright owner(s) are credited and that the original publication in this journal is cited, in accordance with accepted academic practice. No use, distribution or reproduction is permitted which does not comply with these terms.